

Article

Hydrochemistry and Its Controlling Factors of Rivers in the Source Region of the Nujiang River on the Tibetan Plateau

Fuqiang Wang ^{1,2,3}, Yang Zhao ¹, Xi Chen ⁴ and Heng Zhao ^{1,2,*}

¹ School of Water Conservancy, North China University of Water Resources and Electric Power, Zhengzhou 450046, China; wangfuqiang@ncwu.edu.cn (F.W.); yangzhao34@163.com (Y.Z.)

² Collaborative Innovation Center of Water Resources Efficient Utilization and Support Engineering, Zhengzhou 450046, China

³ Henan Key Laboratory of Water Environmental Simulation and Management, Zhengzhou 450046, China

⁴ School of Hydraulic Engineering, Dalian University of Technology, Dalian 116024, China; chenxi218@mail.dlut.edu.cn

* Correspondence: zhaoheng@ncwu.edu.cn; Tel.: +86-137-0371-4660

Received: 28 August 2019; Accepted: 14 October 2019; Published: 17 October 2019



Abstract: The chemical composition of river water collected from the main stream of the Naqu and its tributaries was analyzed to reveal its hydrochemical characteristics and to evaluate the water quality for irrigation purposes. Based on 39 samples, the results revealed mildly alkaline pH values and total dissolved solids (TDS) values ranging from 115 to 676 mg/L, averaging 271 mg/L. Major ion concentrations based on mean values (mg/L) were in the order of $\text{Ca}^{2+} > \text{Na}^+ > \text{Mg}^{2+} > \text{K}^+$ for cations and $\text{HCO}_3^- > \text{SO}_4^{2-} > \text{Cl}^- > \text{CO}_3^{2-}$ for anions. Most hydrochemical types were of the Ca– HCO_3 (~74.36%) type. Cluster analysis (CA) suggested that the hydrochemical characteristics upstream of the main stream of the Naqu were obviously different from those from the middle and downstream of the main stream and its tributaries. The analysis shows that the Sangqu, Basuoqu, Mumuqu, Zongqingqu, Mugequ basin tributary, and the Gongqu basin tributary were mainly affected by carbonate weathering. Carbonate and silicate weathering commonly controlled the hydrochemistry upstream and downstream of the main Naqu, Chengqu, and Mugequ streams. The middle of the main stream of the Naqu was mainly affected by silicate weathering, and anhydrite/gypsum dissolution mainly affected the hydrochemistry of the main Gongqu stream. The quality of water samples was suitable for irrigation purposes, except for one sample from the main stream of the Mugequ.

Keywords: source region of Nujiang river; hydrochemistry; major ions; chemical weathering; Tibetan Plateau

1. Introduction

Rivers are important hubs connecting land and ocean, and they are the main channels for material and energy exchange [1]. The hydrochemical composition of a watershed is indicative of the environment of the area it flows through. An analysis of the hydrochemical composition of a basin can determine the geochemical source of the river solute and related information, including weathering and climate of the watershed [2]. There are many sources of ions in surface water, such as weathering of terrestrial rocks, atmospheric precipitation, and anthropogenic inputs [3].

The Tibetan Plateau is the birthplace of many large rivers, including the Yellow, Yangtze, Ganges–Brahmaputra, Mekong, Salween, and Indus rivers [4]. The hydrochemical characteristics of rivers originating from the Tibetan Plateau are changing with climate change and increasing human activities [5,6]. Due to their role as major resources in Asia, the hydrochemistry of rivers

originating in the Tibetan Plateau have been studied in recent decades [7–14]. However, many previous hydrochemical studies on the headwaters of rivers originating from the Tibetan Plateau have been mainly focused on the Yangtze, Yellow, and Yarlung Tsangpo rivers, and hydrochemical studies on the source region of the Nujiang (Salween) River have been either scarce or based only a few samples [15–22]. A comprehensive analysis of the hydrochemistry of the source region of the Nujiang (Salween) River has not yet been performed. Therefore, in order to clarify the characteristics of the riverine water chemistry in the Naqu River basin, more studies should be carried out.

The Nujiang (Salween) River originates from the Naqu River basin. The Naqu River and its tributaries are major sources for irrigation and are important sources of drinking water for people living in the river basin. In this study, an extensive analysis based on water samples was carried out to characterize the hydrochemistry of the main stream of the Naqu River and its tributaries, and an assessment of water quality for irrigation purposes was conducted.

2. Materials and Methods

2.1. Study Area

The Naqu River basin is located on the eastern Tibetan Plateau, with 16,350 km² of total drainage area from 30°54' to 32°43' N and from 91°12' to 92°54' E (Figure 1). The study area, with an average elevation exceeding 4600 m, is located at the Bangonghu–Nujiang suture. The Naqu River is 460 km long, and the average annual water discharge is 31×10^8 m³ [23]. The major tributaries, Mugequ, Gongqu, and Luoqu, drain into the main stream of the Naqu on the south shore, while Chengqu drains into the main stream of the Naqu on the north shore. The Naqu River basin is located in a semi-humid monsoon climate area in a sub-cold plateau zone, with the mean annual precipitation varying from 317.4 to 477.8 mm, the mean annual potential evaporation varying from 1000 to 1200 mm, and a mean temperature of −2 °C [24]. The precipitation changes greatly during a year, with a rainy season from June to October comprising 81.9% of total annual precipitation [25].

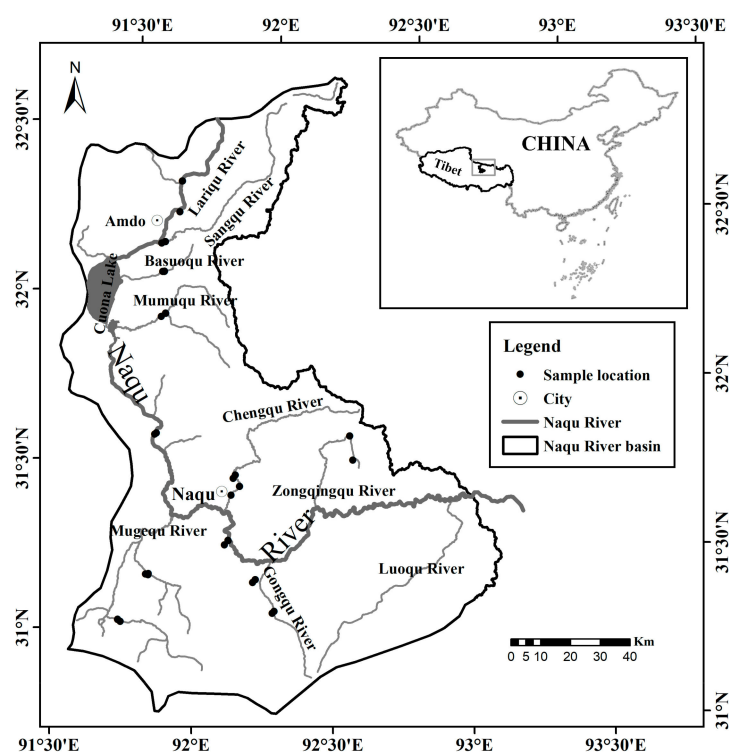


Figure 1. Research area and the distribution of the sampling positions.

The Naqu River basin has abundant grassland resources, which is the basis of animal husbandry development. The grassland area accounts for 73.26% of the basin. In 2013, the total population of the Naqu River basin was 905,000, with a low population density [26]. The distribution of population in the basin increases from upstream to downstream.

The strata of the Naqu River basin are simple. Carboniferous, Jurassic, Tertiary, and Quaternary systems are exposed in the basin [19]. The dominant lithologies are monzonitic granite, granodiorite, quartz diorite, intermediate-acid volcanic rock, volcanic clastic rock, metasandstone, slate, argillaceous sandstone, and sandy conglomerate [27]. In addition, senarmonite, sulphur, and pyrite are also found in the study area [28].

2.2. Sample Collection and Analysis Methods

River water was sampled once a year from 2016 to 2018, on 20–23 August 2016, 20–22 August 2017, and 18–20 August 2018. In all, 39 surface water samples were taken (13 samples each year). The 39 sample sites covered the main channel and tributaries of the Naqu River. The coordinates and altitudes of these sample sites were recorded using a Magellan eXplorist 310 GPS device (Magellan, Santa Clara, CA, USA). Nine samples were taken from the main stream of the Naqu, and 30 samples were taken from tributaries. The sampling sites are shown in Figure 1. Samples were stored in polyethylene bottles that were pre-cleaned with river water. The pH, water temperature, electrical conductivity (EC), and total dissolved solids (TDS) were measured in situ using a Horiba U50 (HORIBA Ltd., Kyoto, Japan). Ca^{2+} , Mg^{2+} , K^{+} , Na^{+} , HCO_3^{-} , CO_3^{2-} , SO_4^{2-} , and Cl^{-} were measured at the laboratory of the No.1 Institute of Geo-environment Survey of Henan, Henan, China. Concentrations of HCO_3^{-} and CO_3^{2-} were measured by titration using 50-mL acid burettes [29]. The concentration of Cl^{-} was determined by titration using 50-mL brown acid burettes [30]. The concentration of SO_4^{2-} was determined by a T9CS double-beam UV/VIS spectrophotometer (Beijing Purkinje General Instrument Co. Ltd., Beijing, China) [31]. Concentrations of Ca^{2+} , Mg^{2+} , K^{+} , and Na^{+} were analyzed by inductive coupled plasma atomic emission spectrometry (ICP-AES) (ICAP 6300, Thermo Fisher Scientific, Waltham, MA, USA) [32].

2.3. Data Processing Methods

Cluster analysis (CA) is an unsupervised pattern-recognition method that is widely applied to analyze water quality [33,34]. Hierarchical and non-hierarchical are the two major categories of CA. Hierarchical cluster analysis starts with each case in a separate cluster, and higher clusters are formed step-by-step until only one cluster remains [35]. To determine the similarity of samples, hierarchical cluster analysis was applied based on standardized data by means of Ward's method with squared Euclidean distances in this study [36]. Parameters selected for hierarchical cluster analysis included Ca^{2+} , Mg^{2+} , K^{+} , Na^{+} , HCO_3^{-} , SO_4^{2-} , Cl^{-} , and TDS.

Triangular plots were applied to classify natural waters in this study [37]. Pearson correlations were performed to evaluate the relationships between ions, TDS, temperature (T), EC, and elevation [38,39]. Gibbs plots have been widely used to analyze factors affecting water chemistry, such as atmospheric precipitation, rock dominance, and the evaporation–crystallization process [40,41]. TDS versus $\text{Na}^{+}/(\text{Na}^{+} + \text{Ca}^{2+})$ or $\text{Cl}^{-}/(\text{Cl}^{-} + \text{HCO}_3^{-})$ was applied to identify the contribution of three end members via the Gibbs schematic diagram.

The suitability of water for irrigation can be known by analyzing dissolved salts. Generally, Na^{+} can replace Ca^{2+} and Mg^{2+} if there is an excess salinity of irrigation water. The displacement reduces the permeability of soil and thus limits the flow of air and water [42]. Sodium percentage (Na%) and sodium adsorption ratio (SAR) (Equations (1) and (2)) were applied to evaluate the suitability of surface water for irrigation [43,44].

$$\text{Na}^{+}\% = \left[(\text{Na}^{+} + \text{K}^{+}) / (\text{Ca}^{2+} + \text{Mg}^{2+} + \text{Na}^{+} + \text{K}^{+}) \right] \times 100 \quad (1)$$

$$\text{SAR} = \text{Na}^+ / \sqrt{(\text{Ca}^{2+} + \text{Mg}^{2+})/2} \quad (2)$$

where concentration is expressed in mEq/L.

Correlation analysis and cluster analysis were carried out using SPSS v 24.0 (IBM, Costa Mesa, CA, USA). Gibbs plots were plotted in Microsoft Excel 2010 (Microsoft Corp., Redmond, WA, USA) and scatter plots of different ions of river water from the Naqu River basin were plotted using Origin 2018 software (OriginLab, Northampton, MA, USA).

3. Results

3.1. Major Elements

The pH was slightly alkaline, varying from 7.50 (GQ03) to 9.02 (NQ02) with an average of 8.21 (Table 1). In terms of spatiotemporal variation, the pH of the middle of the main stream of the Naqu was the highest in the whole catchment every year (2016–2018). The water temperature measured in situ was 9.42–19.02 °C in August 2016, 9.42–17.22 °C in August 2017, and 8.50–18.38 °C in August 2018.

TDS in the whole catchment varied from 115 mg/L (ZQQ02) to 676 mg/L (NQ01), with an average of 271 mg/L. TDS of the upper reach of the main stream of the Naqu River (Lariqu) was the highest in the whole catchment in 2016, 2017, and 2018. Electrical conductivity varied from 156 µS/cm (ZQQ01) to 870 µS/cm (NQ01), averaging 383 µS/cm. TDS and electrical conductivity of the main stream of the Naqu River gradually reduced from upstream to downstream of the main stream (Figure 2). Increasing runoff may have caused this phenomenon. In addition, the electrical conductivity of the upper reach of the main stream of the Naqu was the highest in the whole catchment in 2016, 2017, and 2018, which was in accordance with TDS.

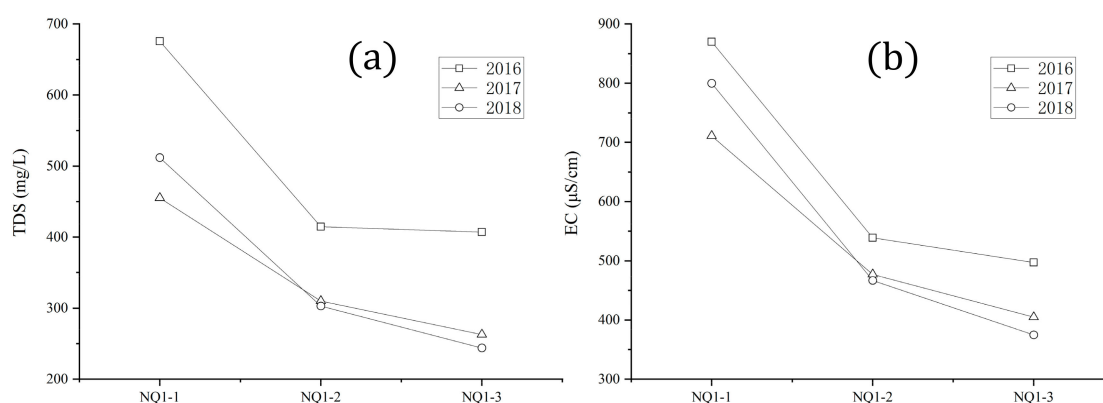


Figure 2. Plots of (a) total dissolved solids (TDS) and (b) electrical conductivity (EC) of the main stream of the Naqu from upstream to downstream. NQ1-1, NQ1-2, NQ1-3: upstream, middle, and downstream of the main stream of the Naqu, respectively.

A comparison with the global mean and other rivers originating from the Tibetan Plateau is presented in Table 1. In terms of TDS values, rivers in the Naqu River basin showed relatively high values (271 ± 138 mg/L) compared to the global mean of 120 mg/L [45,46]. The average TDS value in the whole catchment was similar to the middle and upper segments of the Yarlung Tsangpo draining the Himalayas (~269 mg/L), but lower than that of the Upper Yangze (~778 mg/L), upper Huang He (Yellow) (~394 mg/L), and Upper Mekong (~302 mg/L) rivers [16,17,47,48]. In most water samples, the total cation charge ($\text{TZ}^+ = \text{Na}^+ + \text{K}^+ + 2\text{Mg}^{2+} + 2\text{Ca}^{2+}$) balanced the total anion charge ($\text{TZ}^- = \text{Cl}^- + 2\text{SO}_4^{2-} + 2\text{CO}_3^{2-} + \text{HCO}_3^-$). For the normalized inorganic charge balance ($\text{NICB} = (\text{TZ}^+ - \text{TZ}^-)/\text{TZ}^+$), only three samples had an NICB > 10% in the study.

Major cation concentrations based on mean values (mg/L) in the Naqu River basin were in the following order: $\text{Ca}^{2+} > \text{Na}^+ > \text{Mg}^{2+} > \text{K}^+$. Ca^{2+} comprised 49.71% of TZ^+ and K^+ only accounted

for 1.59% of the total cation charge. The abundance of anions (on a mg basis) in the river water followed the order of $\text{HCO}_3^- > \text{SO}_4^{2-} > \text{Cl}^- > \text{CO}_3^{2-}$. Bicarbonate was the most abundant anion, accounting for 67.87% of TZ^- in the whole catchment in charge equivalent units. SO_4^{2-} made up 48.84–59.43% of TZ^- , with an average of 52.63%, in the main stream of the Gongqu, indicating evaporate dissolution or sulfide oxidation.

3.2. Hydrochemical Type

Hydrochemical type is widely used to analyze characteristics of surface water or groundwater. In this study, the hydrochemical types in the Naqu River basin are presented in Table 2.

Samples from the Naqu River basin were classified based on the triangular plots of major cations and anions (Figure 3). The most frequent hydrochemical type of the Naqu River basin was Ca-HCO_3 (~74.36%). The hydrochemical type upstream of the main stream of the Naqu (Lariqu), Sangqu, Basuoqu, Mumuqu, and Zongqingqu rivers, and the tributary of the Gongqu river was Ca-HCO_3 over the three years of the study (2016–2018). The hydrochemical type in the middle of the main stream of the Naqu was Mg-HCO_3 over the three years, implying that silicate weathering may influence the ionic source of this part of the main stream. The hydrochemical type of the main stream of the Gongqu was Ca-SO_4 over the three years, indicating contributions from evaporates or sulfide minerals.

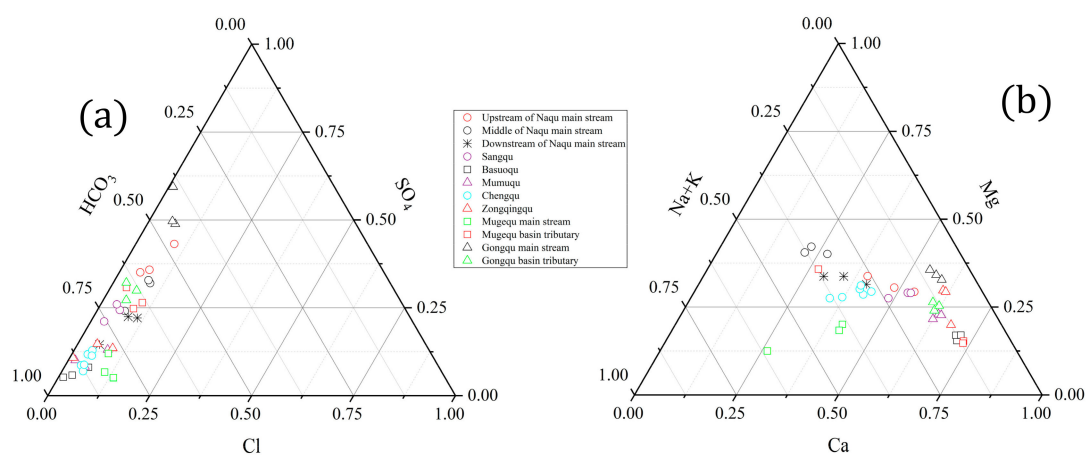


Figure 3. Triangular plots of (a) anions and (b) cations (in equivalent units) of river water from the Naqu River basin.

Table 1. Summary statistics of hydrochemical compositions from the Naqu River and comparisons with other rivers.

River		T	pH	EC ($\mu\text{S}/\text{cm}$)	TDS (mg/L)	K ⁺ (mg/L)	Na ⁺ (mg/L)	Ca ²⁺ (mg/L)	Mg ²⁺ (mg/L)	Cl ⁻ (mg/L)	SO ₄ ²⁻ (mg/L)	HCO ₃ ⁻ (mg/L)	Reference
Naqu, China (n = 39)	Mean	13.14	8.21	382.69	270.57	2.91	24.55	41.64	15.34	9.43	44.78	185.88	This study
	SD	2.83	0.38	174.58	138.19	1.96	17.94	19.62	9.39	6.56	40.51	77.95	
	Min	8.50	7.50	156.00	115.00	0.42	3.75	20.52	4.05	0.46	8.09	52.23	
	Max	19.02	9.02	870.00	675.78	8.30	67.68	92.05	42.03	29.56	181.79	324.08	
Upper Huang He, China	–	–	8.89	–	394	2.56	48.07	33.96	22.70	65.14	20.16	202.95	[17]
Upper Yangtze, China	–	–	7.60	–	778	5.50	157.70	53.40	22.90	233.70	114.90	188.50	[16]
Upper Mekong, China	–	–	8.42	370	302	1	12	49	14	14	69	138	[48]
Yarlung Tangpo, China	–	–	–	–	268.64	1.71	12.98	45.10	8.19	9.53	63.44	116.21	[47]
Global mean	–	–	8	–	120	2.30	6.30	15	4.10	7.80	11.20	58.40	[45,46]

SD, standard deviation; Min, minimum; Max, maximum.

Table 2. Sampling details and hydrochemical type.

Code	River	Location	Elevation (m)	Date (yyyy-mm-dd)	Hydrochemical Type
Main stream of the Naqu					
NQ01	Naqu	Upstream	4714	2016-08-22	Ca-HCO ₃
NQ04	Naqu	Upstream	4771	2017-08-21	Ca-HCO ₃
NQ07	Naqu	Upstream	4764	2018-08-19	Ca-HCO ₃
NQ02	Naqu	Middle	4555	2016-08-22	Mg-HCO ₃
NQ05	Naqu	Middle	4551	2017-08-21	Mg-HCO ₃
NQ08	Naqu	Middle	4546	2018-08-19	Mg-HCO ₃
NQ03	Naqu	Downstream	4463	2016-08-21	Na-HCO ₃
NQ06	Naqu	Downstream	4451	2017-08-22	Ca-HCO ₃
NQ09	Naqu	Downstream	4457	2018-08-20	Ca-HCO ₃
Tributaries					
SQ01	Sangqu	Main stream	4633	2016-08-22	Ca-HCO ₃
SQ02	Sangqu	Main stream	4626	2017-08-21	Ca-HCO ₃
SQ03	Sangqu	Main stream	4631	2018-08-19	Ca-HCO ₃
BSQ01	Basuoqu	Main stream	4727	2016-08-22	Ca-HCO ₃
BSQ02	Basuoqu	Main stream	4712	2017-08-21	Ca-HCO ₃
BSQ03	Basuoqu	Main stream	4712	2018-08-19	Ca-HCO ₃
MMQ01	Mumuqu	Main stream	4625	2016-08-22	Ca-HCO ₃
MMQ02	Mumuqu	Main stream	4622	2017-08-21	Ca-HCO ₃
MMQ03	Mumuqu	Main stream	4619	2018-08-19	Ca-HCO ₃
CQ01	Chengqu	Main stream	4523	2016-08-22	Na-HCO ₃
CQ03	Chengqu	Main stream	4519	2017-08-21	Ca-HCO ₃
CQ05	Chengqu	Main stream	4513	2018-08-19	Ca-HCO ₃
CQ02	Chengqu	Main stream	4497	2016-08-21	Ca-HCO ₃
CQ04	Chengqu	Main stream	4503	2017-08-21	Ca-HCO ₃
CQ06	Chengqu	Main stream	4503	2018-08-19	Ca-HCO ₃
ZQQ01	Zongqingqu	Main stream	4766	2016-08-21	Ca-HCO ₃
ZQQ02	Zongqingqu	Main stream	4567	2017-08-21	Ca-HCO ₃
ZQQ03	Zongqingqu	Main stream	4570	2018-08-19	Ca-HCO ₃
MGQ01	Mugequ	Main stream	4591	2016-08-23	Na-HCO ₃
MGQ03	Mugequ	Main stream	4609	2017-08-20	Ca-HCO ₃
MGQ05	Mugequ	Main stream	4593	2018-08-18	Ca-HCO ₃
MGQ02	Mugequ	Tributary	4708	2016-08-20	Na-HCO ₃
MGQ04	Mugequ	Tributary	4681	2017-08-20	Ca-HCO ₃
MGQ06	Mugequ	Tributary	4687	2018-08-18	Ca-HCO ₃
GQ01	Gongqu	Main stream	4580	2016-08-21	Ca-SO ₄
GQ03	Gongqu	Main stream	4578	2017-08-22	Ca-SO ₄
GQ05	Gongqu	Main stream	4574	2018-08-20	Ca-SO ₄
GQ02	Gongqu	Tributary	4498	2016-08-21	Ca-HCO ₃
GQ04	Gongqu	Tributary	4498	2017-08-22	Ca-HCO ₃
GQ06	Gongqu	Tributary	4487	2018-08-20	Ca-HCO ₃

3.3. Association among the Hydrochemical Attributes

Hierarchical cluster analysis generated a dendrogram (Figure 4), grouping five clusters. Group A comprised CQ01–CQ06, NQ09, MGQ03, and MGQ05. Sample sites of Group A were located at the middle and downstream regions of the Naqu River. TDS of Group A ranged from 137 to 444 mg/L, averaging 277 mg/L. Group B comprised NQ02–NQ03, NQ05–NQ06, NQ08, and MGQ01–MGQ02. Sample sites of Group B were mainly located at the middle and downstream of the main stream of the Naqu. TDS of Group B ranged from 263 to 415 mg/L, averaging 359 mg/L. Group C comprised BSQ01–BSQ03, and SQ01–SQ03. TDS of Group C ranged from 252 to 447 mg/L, averaging 334 mg/L. Sample sites of Group C were located at the upstream region of the Naqu River. A similar environment may be the reason for dividing the Sangqu (SQ01–SQ03) and Basuoqu (BSQ01–BSQ03) into the same cluster. Group D comprised NQ01, NQ04, and NQ07. Group D ranged from 455 to 676 mg/L, averaging 548 mg/L. Sample sites of Group D located upstream the main Naqu. Elevation of sample sites of Group D were higher than other sample sites. TDS of Group D was the highest over the three years of the study. Group E comprised GQ01–GQ06, ZQQ01–ZQQ03, MMQ01–MMQ03, MGQ04, and MGQ06. TDS of Group E ranged from 115 to 195 mg/L, averaging 136 mg/L. Water samples from the same reach

were almost classified into the same cluster, indicating that hydrochemical characteristics of the same reach changed slightly over the three years of the study.

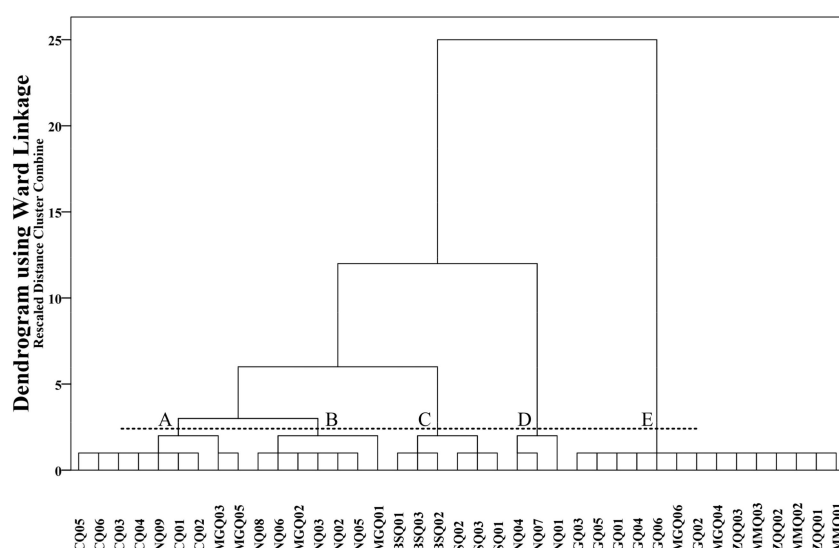


Figure 4. Dendrogram showing clustering of sample sites.

Correlation analysis can establish the relationship between two variables. In this study, correlation coefficients (R) are presented in Table 3. Because the Ca^{2+} – HCO_3^- pair showed high correlation, carbonate weathering may be present in this basin. The correlation of SO_4^{2-} with Mg^{2+} and Ca^{2+} indicates the presence of magnesium sulfate or gypsum/anhydrite. In addition, the high correlation of Na^+ and K^+ implies a common source of two ions most likely associated with silicate weathering. Na^+ , K^+ , and temperature were clearly correlated, suggesting that silicate rock weathering is promoted when temperature increases. The correlation of Ca^{2+} with elevation implies elevation has an important impact on carbonate rock weathering.

Table 3. Pearson correlation of major ions in river water.

	Ca	Mg	K	Na	Cl	HCO_3	SO_4	TDS	T	EC	Elevation
Ca	1										
Mg	0.503 **	1									
K	0.104	0.566 **	1								
Na	0.224	0.750 **	0.937 **	1							
Cl	0.341 *	0.723 **	0.629 **	0.802 **	1						
HCO_3	0.742 **	0.663 **	0.670 **	0.676 **	0.526 **	1					
SO_4	0.554 **	0.791 **	0.150	0.404 *	0.647 **	0.331 *	1				
TDS	0.648 **	0.847 **	0.676 **	0.828 **	0.725 **	0.789 **	0.635 **	1			
T	−0.062	0.328 *	0.547 **	0.583 **	0.257	0.296	−0.078	0.484 **	1		
EC	0.733 **	0.907 **	0.616 **	0.777 **	0.751 **	0.831 **	0.743 **	0.960 **	0.337 *	1	
Elevation	0.563 **	0.051	−0.240	−0.108	0.115	0.167	0.325 *	0.227	−0.109	0.248	1

Correlation is significant at the ** 0.01 and * 0.05 levels. T, temperature.

4. Discussion

4.1. Mechanisms Controlling the Surface Water Chemistry of the Naqu River Basin

Mechanisms including rock weathering, evaporation–crystallization, atmospheric precipitation, and ionic input via human activities control riverine water chemistry [49–52]. In the Naqu River basin, the average population density is 5.5 people/ km^2 , which is very low. Restricted by the natural geographical conditions, the natural economy of animal husbandry is the main occupation in the basin. The total economic volume is small. Thus, human activities have less impact in the Naqu River basin. Natural processes dominate the hydrochemical characteristics of rivers in the Naqu River basin.

From the Gibbs plots, the TDS values in the Naqu River basin fell in the range of 100–700 mg/L (Figure 5). The $\text{Cl}^-/(\text{Cl}^- + \text{HCO}_3^-)$ molar ratio for all samples was <0.5 and the $\text{Na}^+/(\text{Na}^+ + \text{Ca}^{2+})$ molar ratio was <0.5 for 56.4% of samples. All water samples were located in the rock-dominant section shown in Figure 5b. These results indicated the predominance of rock weathering. Rock weathering also dominates the hydrochemical characteristics of the Upper Mekong, Yarlung Tsangpo, and Upper Huang He [17,47,48]. Evaporation–crystallization has an important impact on the Upper Yangtze [16].

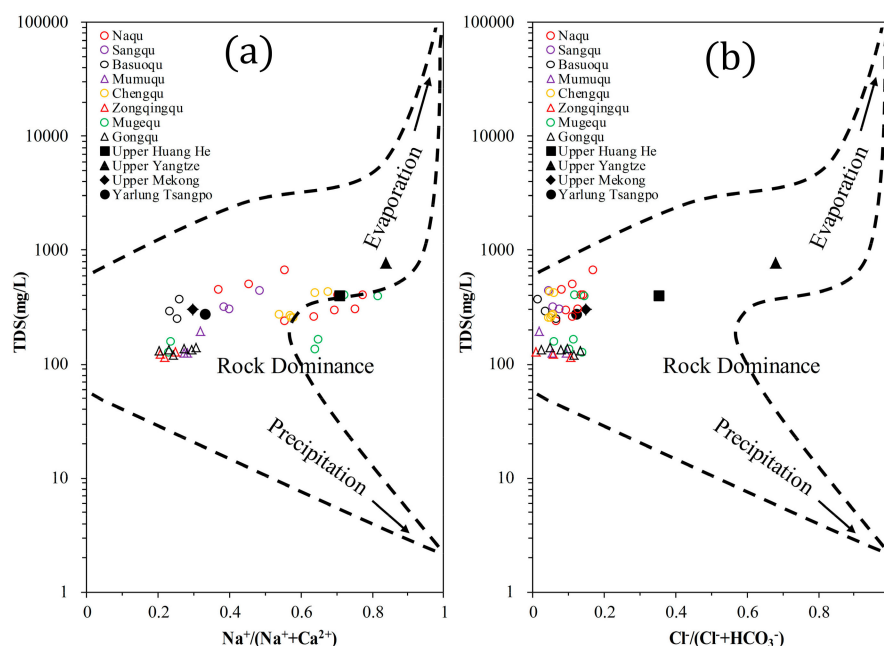


Figure 5. Gibbs plots of river water of the Naqu River basin. (a) TDS versus $\text{Na}^+ / (\text{Na}^+ + \text{Ca}^{2+})$; (b) TDS versus $\text{Cl}^- / (\text{Cl}^- + \text{HCO}_3^-)$.

The molar ratios of $\text{Na}^+ / \text{Cl}^-$ and K^+ / Cl^- were 0.8517 and 0.0176, respectively, in marine aerosol, while their average molar ratios were 4.68 and 0.35, respectively, in the study area. Larger differences between water samples from the study area and marine aerosol in these ratios indicate that atmospheric inputs contribute little to the Naqu River basin. The result is consistent with a previous study [53]. The ionic relationships of water samples from the river basin are shown in Table 4.

4.2. Chemical Weathering

Chemical weathering is an important source of major ions in river water. The chemical weathering of different rocks yields different combinations of dissolved cations and anions [54,55]. For instance, Ca^{2+} and Mg^{2+} mainly derive from carbonate and silicate weathering and evaporate dissolution, and Na^+ and K^+ are contributed by evaporate dissolution and silicate weathering [56]. For anions, SO_4^{2-} and Cl^- derive from evaporate dissolution or sulfide oxidation. Carbonate weathering and silicate weathering can contribute HCO_3^- [57].

The $\text{HCO}_3^- / (\text{HCO}_3^- + \text{SO}_4^{2-})$ ratio can identify carbonic acid-mediated reactions. The ratio is more than 0.5 if the carbonic acid-mediated reaction is more important than evaporate dissolution (anhydrite/gypsum, sodium sulfate) or sulfide oxidation. All samples fell in Area 1 except samples of the main stream of the Gongqu, implying the leading role of carbonic acid-mediated reactions in these rivers except for the main stream of the Gongqu (Figure 6a).

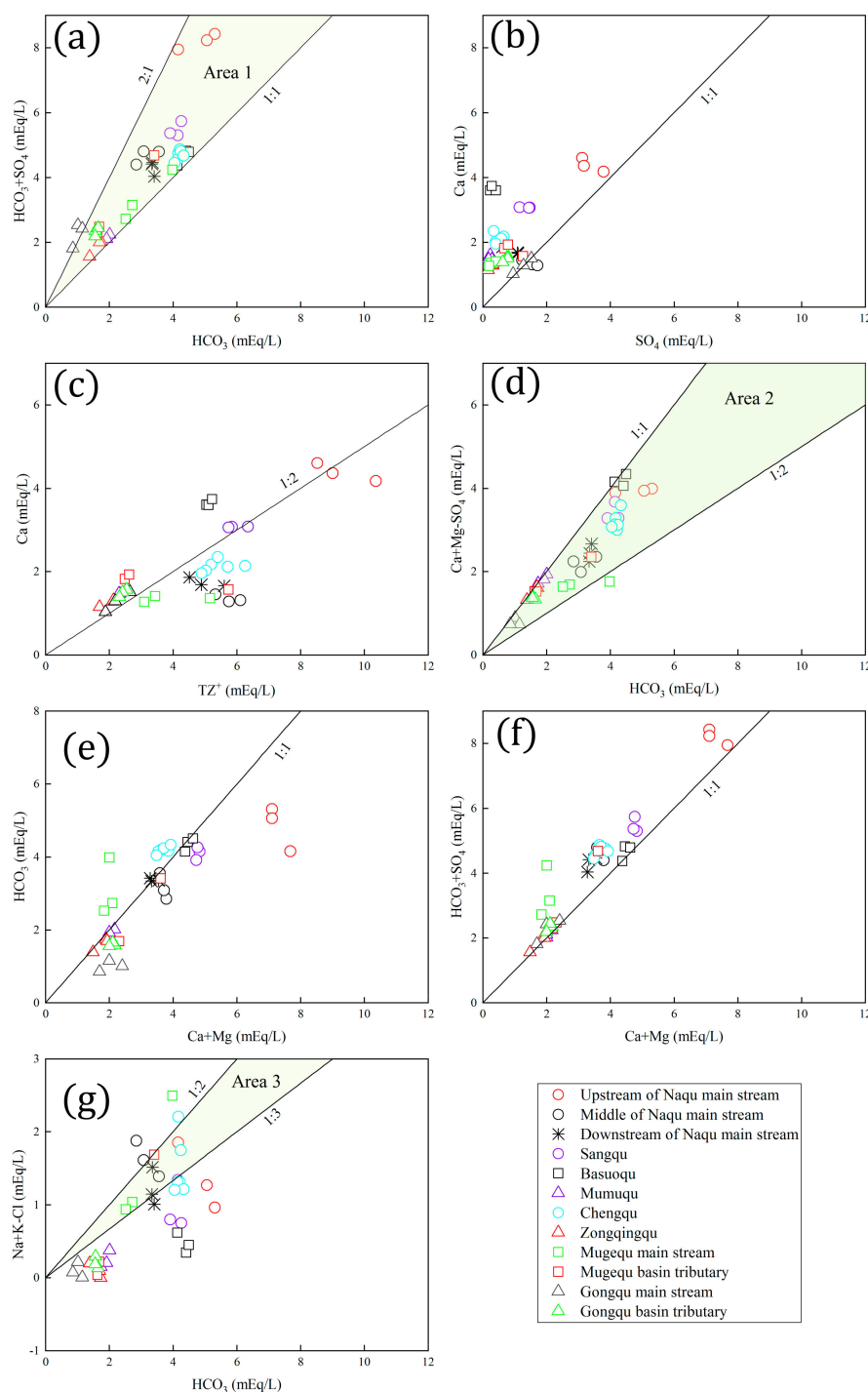


Figure 6. Scatter plots of ions of river water from the Naqu River basin. (a) $\text{HCO}_3 + \text{SO}_4$ and HCO_3 ; (b) Ca and SO_4 ; (c) Ca and TZ^+ ; (d) $(\text{Ca} + \text{Mg} - \text{SO}_4)$ and HCO_3 ; (e) HCO_3 and $(\text{Ca} + \text{Mg})$; (f) $(\text{HCO}_3 + \text{SO}_4)$ and $(\text{Ca} + \text{Mg})$; (g) $(\text{Na} + \text{K} - \text{Cl})$ and HCO_3 .

In general, carbonates are more easily weathered than silicates [58]. The high mean ratios of $(\text{Ca}^{2+} + \text{Mg}^{2+})/(\text{Na}^+ + \text{K}^+)$ and $\text{HCO}_3^-/(\text{Na}^+ + \text{K}^+)$ suggest that the Sangqu, Basuoqu, Mumuqu, and Zongqingqu rivers, and the Mugequ and Gongqu basin tributaries, flow through regions characterized by carbonate weathering (Table 4). Samples from these sources almost clustered along the 1:1 line, which also confirms the leading role of carbonate weathering in these rivers (Figure 6e).

The ratio of $(\text{Ca}^{2+} + \text{Mg}^{2+} - \text{SO}_4^{2-})/\text{HCO}_3^-$ can distinguish between carbonate and silicate weathering to some extent, but it may overestimate the contribution of evaporite dissolution. One sample from the main stream of the Mugequ fell below the 1:2 line, and two samples fell in Area 2, suggesting that carbonate weathering is very important to the main Mugequ (Figure 6d). The ratio of $(\text{Na}^+ + \text{K}^+ - \text{Cl}^-)/\text{HCO}_3^-$ can identify silicate weathering to some extent. Two samples from the main stream of the Mugequ fell in Area 3, and one sample fell above the 1:2 line (Figure 6g). These phenomena suggests that carbonate and silicate weathering commonly control the hydrochemistry of the main Mugequ. Samples of the Chengqu fell in Area 2 (Figure 6d). One sample of the Chengqu fell above the 1:2 line, one sample fell in Area 3, and other samples clustered along the 1:3 line (Figure 6g). This suggests that carbonate and silicate weathering commonly control the hydrochemistry of the Chengqu.

One sample upstream the main Naqu fell in Area 3, and two samples fell below the 1:3 line (Figure 6g). As shown in Figure 6d, samples from upstream the main Naqu (Lariqu) fell in Area 2. This suggests that upstream the main Naqu is controlled by carbonate and silicate weathering. Two samples from the middle of the main stream of the Naqu fell above the 1:2 line, and one sample fell in Area 3, implying the leading role of silicate weathering (Figure 6g). Samples from downstream the main Naqu fell in Area 2 (Figure 6d). Two samples from downstream the main Naqu fell in Area 3, and one sample fell below the 1:3 line (Figure 6g). This implies that the hydrochemistry downstream the main Naqu is controlled by carbonate and silicate weathering.

The $\text{Ca}^{2+}/\text{SO}_4^{2-}$ ratio can distinguish between anhydrite/gypsum dissolution and pyrite oxidation. The ratio is 1 if anhydrite/gypsum dissolution occurs [59]. Samples of the main stream of the Gongqu clustered along the 1:1 line, indicating that anhydrite/gypsum dissolution rather than pyrite oxidation contributed sulfate ion (Figure 6b). Almost all samples from the main stream of the Gongqu fell above the 1:2 line, indicating the dominance of Ca^{2+} in TZ^+ (Figure 6c). Furthermore, these phenomena imply a leading role of anhydrite/gypsum in the main stream of the Gongqu. The ratios of $\text{Ca}^{2+}/\text{SO}_4^{2-}$ upstream of the main Naqu (Lariqu) ranged from 1.10 to 1.48, with an average of 1.32, suggesting that sulfuric acid may be from anhydrite/gypsum dissolution (Figure 6b).

Table 4. Ionic ratios of various hydrochemical attributes of river water from the Naqu River basin.

Parameter		NQ1-1	NQ1-2	NQ1-3	SQ	BSQ	MMQ	CQ	ZQQ	MGQ 1-1	MGQ 2-1	GQ1-1	GQ2-1	Naqu River Basin
Na ⁺ /Cl [−]	Mean	2.96	4.69	4.02	5.07	5.91	4.59	7.29	5.77	4.03	2.83	3.70	2.74	4.68
	Min	2.87	4.45	3.55	3.04	1.98	1.63	5.32	0.87	3.60	1.04	0.91	1.57	0.82
	Max	3.10	4.97	4.94	7.87	12.08	9.63	11.36	14.73	4.43	4.52	8.71	4.44	14.73
K ⁺ /Cl [−]	Mean	0.16	0.27	0.28	0.33	0.37	0.46	0.61	0.59	0.31	0.20	0.23	0.20	0.35
	Min	0.12	0.26	0.21	0.21	0.14	0.19	0.42	0.09	0.30	0.09	0.10	0.13	0.09
	Max	0.19	0.28	0.41	0.48	0.70	0.90	0.93	1.46	0.32	0.28	0.42	0.28	1.46
(Ca ²⁺ +Mg ²⁺)/(Na ⁺ +K ⁺)	Mean	3.87	1.84	2.17	4.08	7.07	5.95	2.22	8.92	1.22	5.52	10.18	6.40	4.74
	Min	2.86	1.63	1.72	3.17	6.58	5.25	1.61	7.07	0.64	1.70	9.26	5.92	0.64
	Max	4.99	2.06	2.65	4.64	7.75	6.44	2.68	10.10	1.57	7.60	11.12	6.93	11.12
HCO ₃ [−] /(Na ⁺ +K ⁺)	Mean	2.65	1.59	2.18	3.50	6.85	5.46	2.53	8.05	1.77	4.17	5.11	4.87	3.94
	Min	1.55	1.23	1.63	2.72	6.21	4.88	1.74	6.61	1.26	1.60	4.27	4.26	1.23
	Max	3.73	2.04	2.76	3.95	7.53	6.20	2.95	8.83	2.04	5.63	6.39	5.42	8.83

¹NQ1-1, NQ1-2, NQ1-3: upstream, middle, and downstream of the main stream of the Naqu, respectively; SQ: Sangqu; BSQ: Basuoqu; MMQ: Mumuqu; CQ: Chengqu; ZQQ: Zongqingqu; MGQ1-1, MGQ2-1: main stream and basin tributary of the Mugequ, respectively; GQ1-1, GQ2-1: main stream and basin tributary of the Gongqu, respectively. ²Na⁺/Cl[−] and K⁺/Cl[−] ratios derived from the molar; (Ca²⁺+Mg²⁺)/(Na⁺+K⁺) and HCO₃[−]/(Na⁺+K⁺) ratios derived from the charge equivalent.

4.3. Suitability for Irrigation Quality

Restricted by physical geography and geographical conditions, the natural economy of animal husbandry is the main occupation in the Naqu River basin. Irrigation grasslands in the Naqu River basin are all self-flowing, directly diverting water from rivers. As it is a major water resource for irrigation, a water quality evaluation of the Naqu River basin was carried out in the present study.

The values of $\text{Na}^+\%$ and SAR in the Naqu River basin are presented in Table 5, and the classification of water quality for irrigation purposes is presented in Table 6. The suitability of water for irrigation according to $\text{Na}^+\%$ values is based on five classes: “excellent” if $\text{Na}^+\%$ values are less than 20, “good” if values range between 20 and 40, “permissible” if values range between 40 and 60, “doubtful” if values range between 60 and 80, and “unsuitable” if $\text{Na}^+\%$ values exceed 80 [60]. For the whole study area, the water quality was good for irrigation, because the average value of $\text{Na}^+\%$ in the Naqu River basin was 22.96 ± 12.31 (range 8.25–61.13). In terms of spatial variation, the average value of $\text{Na}^+\%$ in the Mugequ main stream was the highest (mean 46.90 ± 12.35). For Zongqingqu, the water quality was excellent for irrigation because the average value of $\text{Na}^+\%$ was the lowest (mean 10.28 ± 1.84). Based on $\text{Na}^+\%$ values, the “excellent for irrigation” category comprised 51.28%, “good” comprised 43.59%, “permissible” comprised 2.56%, and “doubtful” comprised 2.56% of all samples. For the water samples from the main stream of the Mugequ (MGQ01, MGQ03, MGQ05), the sodium percentage was higher than in other samples. Therefore, the water resources from the main stream of the Mugequ should be utilized cautiously for irrigation.

The suitability of water for irrigation according to SAR values is based on four classes: “excellent for irrigation” if SAR values are less than 10, “good” if values range between 10 and 18, “fair” if values range between 18 and 26, and “poor” if SAR values exceed 26 [60]. In present study, all SAR values were less than 3, and the grand mean value was 0.81 ± 0.59 . The mean SAR value in the main stream of the Mugequ was the highest (mean 1.79 ± 1.00), while the main stream of the Zongqingqu was the lowest (mean 0.19 ± 0.02), which is consistent with the $\text{Na}^+\%$ values. Therefore, the quality of all water samples fell in the suitable range, except one sample from the main stream of the Mugequ, based on SAR and $\text{Na}^+\%$.

Table 5. Water quality for irrigation purposes, Naqu River basin.

Parameter		NQ1-1	NQ1-2	NQ1-3	SQ	BSQ	MMQ	CQ	ZQQ	MGQ1-1	MGQ2-1	GQ1-1	GQ2-1	Naqu River Basin
SAR	Mean	0.99	1.41	1.16	0.73	0.40	0.31	1.17	0.19	1.79	0.67	0.18	0.30	0.81
	SD	0.31	0.19	0.28	0.17	0.03	0.05	0.26	0.02	1.00	0.71	0.02	0.03	0.59
	Min	0.71	1.23	0.89	0.62	0.37	0.28	0.97	0.17	1.21	0.25	0.16	0.27	0.16
	Max	1.32	1.60	1.46	0.92	0.43	0.36	1.60	0.22	2.94	1.49	0.21	0.33	2.94
Na%	Mean	21.21	35.39	31.98	20.05	12.44	14.48	31.48	10.28	46.90	20.25	8.98	13.56	22.96
	SD	4.62	2.66	4.66	3.40	0.91	1.36	4.30	1.84	12.35	14.52	0.75	0.93	12.31
	Min	16.69	32.67	27.39	17.73	11.43	13.43	27.20	9.01	38.96	11.63	8.25	12.61	8.25
	Max	25.92	37.98	36.71	23.95	13.20	16.01	38.36	12.39	61.13	37.01	9.75	14.45	61.13

¹NQ1-1, NQ1-2, NQ1-3: upstream, middle, and downstream of the main stream of the Naqu, respectively; SQ: Sangqu; BSQ: Basuoqu; MMQ: Mumuqu; CQ: Chengqu; ZQQ: Zongqingqu; MGQ1-1, MGQ2-1: main stream and basin tributary of the Mugequ, respectively; GQ1-1, GQ2-1: main stream and basin tributary of the Gongqu, respectively. ²SD, standard deviation; Min, minimum; Max, maximum.

Table 6. Classification scheme based on suitability of water for irrigation, Naqu River basin.

Parameter	Threshold	Class	NQ1-1	NQ1-2	NQ1-3	SQ	BSQ	MMQ	CQ	ZQQ	MGQ1-1	MGQ2-1	GQ1-1	GQ2-1
SAR	<10	Excellent	3	3	3	3	3	3	6	3	3	3	3	3
	10–18	Good	–	–	–	–	–	–	–	–	–	–	–	–
	18–26	Fair	–	–	–	–	–	–	–	–	–	–	–	–
	>26	Poor	–	–	–	–	–	–	–	–	–	–	–	–
Na%	<20	Excellent	1	–	–	2	3	3	–	3	–	2	3	3
	20–40	Good	2	3	3	1	–	–	6	–	1	1	–	–
	40–60	Permissible	–	–	–	–	–	–	–	–	1	–	–	–
	60–80	Doubtful	–	–	–	–	–	–	–	–	1	–	–	–
	>80	Unsuitable	–	–	–	–	–	–	–	–	–	–	–	–

NQ1-1, NQ1-2, NQ1-3: upstream, middle, downstream of the main stream of the Naqu, respectively; SQ: Sangqu; BSQ: Basuoqu; MMQ: Mumuqu; CQ: Chengqu; ZQQ: Zongqingqu; MGQ1-1, MGQ2-1: main stream and tributary of the Mugequ, respectively; GQ1-1, GQ2-1: main stream and tributary of the Gongqu, respectively.

5. Conclusions

Based on 39 samples (13 samples each year) from the main stream of the Naqu and its tributaries, this study analyzed the hydrochemical characteristics of river water. The weathering process and water quality for irrigation were also discussed in the study.

The analysis shows that the prevailing water facies was a Ca-HCO₃ (~74.36%) type in the main stream of the Naqu and its tributaries. Cluster analysis suggests that the hydrochemical characteristics upstream of the main stream of the Naqu were obviously different from the middle and downstream and tributaries.

The Sangqu, Basuoqu, Mumuqu, and Zongqingqu rivers and the Mugequ and the Gongqu basin tributaries flow through regions characterized by carbonate weathering. The middle of the main stream of the Naqu is mainly affected by silicate weathering. Carbonate and silicate weathering control the hydrochemistry upstream and downstream of the main stream of the Naqu, Chengqu, and Mugequ rivers. Anhydrite/gypsum dissolution makes the most important contribution to main stream of the Gongqu.

The overall water quality of the Naqu River basin samples were suitable for irrigation purposes, except for one sample from the main stream of the Mugequ.

Author Contributions: Conceptualization, F.W.; Formal analysis, Y.Z.; Funding acquisition, F.W.; Investigation, F.W., Y.Z., and X.C.; Methodology, Y.Z. and X.C.; Supervision, F.W. and H.Z.; Visualization, H.Z.; Writing—original draft, F.W. and Y. Z.; Writing—review & editing, F.W., Y.Z., and H.Z. F.W. and H.Z. guided and supervised the whole process; and all authors read and approved the final manuscript.

Funding: This work was supported by the National Natural Science Foundation of the People's Republic of China (51879106; 51709111), the Major Research Plan of the National Natural Science Foundation of China (91547209), the National Key Research and Development Program of China (2016YFC0401401), the Distinguished Young Scholar of Science and Technology Innovation (184100510014), and the Science and Technology Innovation Team in Universities of Henan Province (20IRTSTHN010).

Acknowledgments: The authors would like to express their sincere gratitude to the anonymous reviewers for their constructive comments and useful suggestions that helped us improve our paper.

Conflicts of Interest: No conflict of interest exists in the submission of this manuscript, and the manuscript is approved by all authors for publication.

References

1. Xu, S.; Li, S.L.; Zhong, J.; Su, J.; Chen, S. Hydrochemical characteristics and chemical weathering processes in Chishui River Basin. *Chin. J. Ecol.* **2018**, *37*, 667–678.
2. An, Y.L.; Lv, J.M.; Luo, J.; Wu, Q.X.; Jiang, H.; Peng, W.B.; Yu, X. Hydro-chemical Characteristics of Upper Chishui River Basin in Dry Season. *Environ. Sci. Technol.* **2015**, *38*, 117–122.
3. Moon, S.; Huh, Y.; Qin, J.; van Pho, N. Chemical weathering in the Hong (Red) River basin: Rates of silicate weathering and their controlling factors. *Geochim. Cosmochim. Acta* **2007**, *71*, 1411–1430. [[CrossRef](#)]
4. Li, Z.; Yu, G.; Xu, M.; Hu, X.; Yang, H.; Hu, S. Progress in studies on river morphodynamics in Qinghai-Tibet Plateau. *Adv. Water Sci.* **2016**, *27*, 617–628.
5. Zhang, Y.; Sillanpää, M.; Li, C.; Guo, J.; Qu, B.; Kang, S. River water quality across the Himalayan regions: elemental concentrations in headwaters of Yarlung Tsangbo, Indus and Ganges River. *Environ. Earth Sci.* **2015**, *73*, 4151–4163. [[CrossRef](#)]
6. Zhang, F.; Kaiser, F.-u.-R.; Zeng, C.; Pant, R.R.; Wang, G.; Zhang, H.; Chen, D. Meltwater hydrochemistry at four glacial catchments in the headwater of Indus River. *Environ. Sci. Pollut. Res.* **2019**, *26*, 23645–23660. [[CrossRef](#)]
7. Sarin, M.M.; Krishnaswami, S. Major ion chemistry of the Ganga—Brahmaputra river systems, India. *Nature* **1984**, *312*, 538–541. [[CrossRef](#)]
8. Hodson, A.; Porter, P.; Lowe, A.; Mumford, P. Chemical denudation and silicate weathering in Himalayan glacier basins: Batura Glacier, Pakistan. *J. Hydrol.* **2002**, *262*, 193–208. [[CrossRef](#)]
9. West, A.J.; Bickle, M.J.; Collins, R.; Brasington, J. Small-catchment perspective on Himalayan weathering fluxes. *Geology* **2002**, *30*, 355–358. [[CrossRef](#)]

10. Hren, M.T.; Chamberlain, C.P.; Hilley, G.E.; Blisniuk, P.M.; Bookhagen, B. Major ion chemistry of the Yarlung Tsangpo-Brahmaputra river: Chemical weathering, erosion, and CO₂ consumption in the southern Tibetan plateau and eastern syntaxis of the Himalaya. *Geochim. Cosmochim. Acta* **2007**, *71*, 2907–2935. [[CrossRef](#)]
11. Liu, C.Q.; Zhao, Z.Q.; Tao, F.; Li, S.L. Chemical weathering of Qinghai-Tibet Plateau: geochemical study of Jinsha Jiang, Lancang Jiang, and Nu Jiang river water, China. *Geochim. Cosmochim. Acta Suppl.* **2008**, *72*, 556.
12. Li, S.L.; Chetelat, B.; Yue, F.J.; Zhao, Z.Q.; Liu, C.Q. Chemical weathering processes in the Yalong River draining the eastern Tibetan Plateau, China. *J. Asian Earth Sci.* **2014**, *88*, 74–84. [[CrossRef](#)]
13. Qu, B.; Zhang, Y.; Kang, S.; Sillanpaa, M. Water quality in the Tibetan Plateau: Major ions and trace elements in rivers of the “Water Tower of Asia”. *Sci. Total Environ.* **2019**, *649*, 571–581. [[CrossRef](#)] [[PubMed](#)]
14. Ghezzi, L.; Iaccarino, S.; Carosi, R.; Montomoli, C.; Simonetti, M.; Paudyal, K.R.; Cidu, R.; Petrini, R. Water quality and solute sources in the Marsyangdi River system of Higher Himalayan range (West-Central Nepal). *Sci. Total Environ.* **2019**, *677*, 580–589. [[CrossRef](#)] [[PubMed](#)]
15. Wu, W.; Yang, J.; Xu, S.; Yin, H. Geochemistry of the headwaters of the Yangtze River, Tongtian He and Jinsha Jiang: Silicate weathering and CO₂ consumption. *Appl. Geochem.* **2008**, *23*, 3712–3727. [[CrossRef](#)]
16. Jiang, L.; Yao, Z.; Liu, Z.; Wang, R.; Wu, S. Hydrochemistry and its controlling factors of rivers in the source region of the Yangtze River on the Tibetan Plateau. *J. Geochem. Explor.* **2015**, *155*, 76–83. [[CrossRef](#)]
17. Wu, L.; Huh, Y.; Qin, J.; Du, G.; van Der Lee, S. Chemical weathering in the Upper Huang He (Yellow River) draining the eastern Qinghai-Tibet Plateau. *Geochim. Cosmochim. Acta* **2005**, *69*, 5279–5294. [[CrossRef](#)]
18. Liu, J.; Zhao, Y.; Li, Z.; Guo, H. Quantitative source apportionment of water solutes and CO₂ consumption of the whole Yarlung Tsangpo River basin in Tibet, China. *Environ. Sci. Pollut. Res. Int.* **2019**, *26*, 1–13. [[CrossRef](#)]
19. Wu, W.; Xu, S.; Yang, J.; Yin, H. Silicate weathering and CO₂ consumption deduced from the seven Chinese rivers originating in the Qinghai-Tibet Plateau. *Chem. Geol.* **2008**, *249*, 307–320. [[CrossRef](#)]
20. Noh, H.; Huh, Y.; Qin, J.; Ellis, A. Chemical weathering in the Three Rivers region of Eastern Tibet. *Geochim. Cosmochim. Acta* **2009**, *73*, 1857–1877. [[CrossRef](#)]
21. Tao, Z.H.; Zhao, Z.Q.; Zhang, D.; Li, X.D.; Liu, C.Q. Chemical weathering in the three rivers (Jingshajiang, Lancangjiang, and Nujiang) Watershed, Southwest China. *Chin. J. Ecol.* **2015**, *34*, 2297–2308.
22. Zhang, L.L.; Zhao, Z.Q.; Zhang, W.; Tao, Z.H.; Huang, L.; Yang, J.X.; Wu, Q.X.; Liu, C.Q. Characteristics of water chemistry and its indication of chemical weathering in Jinshajiang, Lancangjiang and Nujiang drainage basins. *Environ. Earth Sci.* **2016**, *75*, 506. [[CrossRef](#)]
23. Yan, D.; Liu, S.; Qin, T.; Weng, B.; Li, C.; Lu, Y.; Liu, J. Evaluation of TRMM precipitation and its application to distributed hydrological model in Naqu River Basin of the Tibetan Plateau. *Hydrol. Res.* **2016**, *48*, 822–839. [[CrossRef](#)]
24. Liu, S.; Yan, D.; Qin, T.; Weng, B.; Lu, Y.; Dong, G.; Gong, B. Precipitation phase separation schemes in the Naqu River basin, eastern Tibetan plateau. *Theor. Appl. Climatol.* **2018**, *131*, 399–411. [[CrossRef](#)]
25. Chen, X.; Wang, G.; Wang, F. Classification of Stable Isotopes and Identification of Water Replenishment in the Naqu River Basin, Qinghai-Tibet Plateau. *Water* **2019**, *11*, 46. [[CrossRef](#)]
26. Lu, Y.J. Interaction and Joint Regulation between Water and Soil Resources in the Alpine Region: A Case Study in the Naqu River Basin of the Tibetan Plateau. Ph.D. Thesis, China Institute of Water Resources & Hydropower Research (IWH), Beijing, China, May 2017.
27. Sun, S.J.; Zhang, L.P.; Ding, X.; Sun, W.D.; Zhang, Z.R. Zircon U-Pb ages, Hf isotopes and geochemical characteristics of volcanic rocks in Nagqu area, Tibet and their petrogenesis. *Acta Petrol. Sin.* **2015**, *31*, 2063–2077.
28. Luo, M.; Pan, F.C.; Li, J.C.; Xu, Z.Z.; Deng, W.Z.; Li, G.Q.; Liu, L.J. Greatgandise Northern Tibet Metallogenic Series Study of Ore Deposits. *Acta Petrol. Sin.* **2015**, *89*, 715–730.
29. Ministry of Geology and Mineral Resources of the People’s Republic of China. *Testing Methods of Underground Water Quality—Determination of Carbonate, Bicarbonate and Hydroxide-Titrimetric (DZ/T0064.49-93)*; China Standards Press: Beijing, China, 1993.
30. Ministry of Geology and Mineral Resources of the People’s Republic of China. *Testing Methods of Underground Water Quality—Determination of Chloride-Aargentometric Titration (DZ/T0064.50-93)*; China Standards Press: Beijing, China, 1993.

31. Ministry of Geology and Mineral Resources of the People's Republic of China. *Testing Methods of Underground Water Quality—Determination of Sulfate-Turbidimetry (DZ/T0064.65-93)*; China Standards Press: Beijing, China, 1993.
32. Ministry of Environmental Protection of the People's Republic of China. *Water Quality—Determination of 32 Elements—Inductively Coupled Plasma Optical Emission Spectrometry (HJ776-2015)*; China Environmental Sciences Press: Beijing, China, 2015.
33. Zhang, Y.; Guo, F.; Meng, W.; Wang, X.Q. Water quality assessment and source identification of Daliao river basin using multivariate statistical methods. *Environ. Monit. Assess.* **2008**, *152*, 105. [[CrossRef](#)]
34. Zhao, L.; Li, W.; Lin, L.; Guo, W.; Zhao, W.; Tang, X.; Gong, D.; Li, Q.; Xu, P. Field Investigation on River Hydrochemical Characteristics and Larval and Juvenile Fish in the Source Region of the Yangtze River. *Water* **2019**, *11*, 1342. [[CrossRef](#)]
35. Zhang, X.; Wang, Q.; Liu, Y.; Wu, J.; Yu, M. Application of multivariate statistical techniques in the assessment of water quality in the Southwest New Territories and Kowloon, Hong Kong. *Environ. Monit. Assess.* **2011**, *173*, 17–27. [[CrossRef](#)]
36. Zhao, J.; Fu, G.; Lei, K.; Li, Y. Multivariate analysis of surface water quality in the Three Gorges area of China and implications for water management. *J. Environ. Sci.* **2011**, *23*, 1460–1471. [[CrossRef](#)]
37. Vespasiano, G.; Apollaro, C.; De Rosa, R.; Muto, F.; Larosa, S.; Fiebig, J.; Mulch, A.; Marini, L. The Small Spring Method (SSM) for the definition of stable isotope–elevation relationships in Northern Calabria (Southern Italy). *Appl. Geochem.* **2015**, *63*, 333–346. [[CrossRef](#)]
38. Zhang, L.; Song, X.; Xia, J.; Yuan, R.; Zhang, Y.; Liu, X.; Han, D. Major element chemistry of the Huai River basin, China. *Appl. Geochem.* **2011**, *26*, 293–300. [[CrossRef](#)]
39. Kobus, S.; Glińska-Lewczuk, K.; Sidoruk, M.; Skwierawski, A.; Obolewski, K.; Timofte, C.M.; Sowiński, P. Effect of hydrological connectivity on physicochemical properties of bottom sediments of floodplain lakes—A case study of the Łyna River, Northern Poland. *Environ. Eng. Manag. J.* **2016**, *15*, 1237–1246. [[CrossRef](#)]
40. Gibbs, R.J. Mechanisms Controlling World Water Chemistry. *Science* **1970**, *170*, 1088–1090. [[CrossRef](#)]
41. Feth, J.H.; Gibbs, R.J. Mechanisms Controlling World Water Chemistry: Evaporation-Crystallization Process. *Science* **1971**, *172*, 870–872. [[CrossRef](#)]
42. Ndoye, S.; Fontaine, C.; Gaye, C.B.; Razack, M. Groundwater Quality and Suitability for Different Uses in the Saloum Area of Senegal. *Water* **2018**, *10*, 1837. [[CrossRef](#)]
43. Richards, L. *Diagnosis and Improvement of Saline and Alkali Soils*; Handbook No. 60; US Department of Agriculture: Washington, DC, USA, 1954.
44. Kumar, M.; Kumari, K.; Ramanathan, A.; Saxena, R. A comparative evaluation of groundwater suitability for irrigation and drinking purposes in two intensively cultivated districts of Punjab, India. *Environ. Geol.* **2007**, *53*, 553–574. [[CrossRef](#)]
45. Gaillardet, J.; Dupré, B.; Louvat, P.; Allègre, C.J. Global silicate weathering and CO₂ consumption rates deduced from the chemistry of large rivers. *Chem. Geol.* **1999**, *159*, 3–30. [[CrossRef](#)]
46. Meybeck, M. *Global Occurrence of Major Elements in Rivers*; Pergamon: Oxford, UK, 2003.
47. Jiang, L.G.; Yao, Z.J.; Wang, R.; Liu, Z.F.; Wang, L.; Wu, S.S. Hydrochemistry of the middle and upper reaches of the Yarlung Tsangpo River system: Weathering processes and CO₂ consumption. *Environ. Earth Sci.* **2015**, *74*, 2369–2379. [[CrossRef](#)]
48. Huang, X.; Sillanpää, M.; Gjessing, E.T.; Vogt, R.D. Water quality in the Tibetan Plateau: Major ions and trace elements in the headwaters of four major Asian rivers. *Sci. Total Environ.* **2009**, *407*, 6242–6254. [[CrossRef](#)] [[PubMed](#)]
49. Apollaro, C.; Marini, L.; De Rosa, R.; Settembrino, P.; Scarciglia, F.; Vecchio, G. Geochemical features of rocks, stream sediments, and soils of the Fiume Grande Valley (Calabria, Italy). *Env. Geol.* **2007**, *52*, 719–729. [[CrossRef](#)]
50. Bloise, A.; Belluso, E.; Critelli, T.; Catalano, M.; Apollaro, C.; Miriello, D.; Barrese, E. Amphibole asbestos and Other Fibrous Minerals in the Meta-Basalt of the Gimigliano-Mount Reventino Unit (Calabria, south-Italy). *Rendiconti Online della Società Geologica Italiana* **2012**, *21*, 847–848.
51. Perri, F.; Ietto, F.; Le Pera, E.; Apollaro, C. Weathering processes affecting granitoid profiles of Capo Vaticano (Calabria, southern Italy) based on petrographic, mineralogic and reaction path modelling approaches. *Geol. J.* **2016**, *51*, 368–386. [[CrossRef](#)]

52. Gao, Q.Z.; Tao, Z.; Huang, X.; Nan, L.; Yu, K.; Wang, Z. Chemical weathering and CO₂ consumption in the Xijiang River basin, South China. *Geomorphology* **2009**, *106*, 324–332. [[CrossRef](#)]
53. Zhang, D.; Shi, C.; La, J. A study of chemical properties of rains on the Tibetan Plateau. *Acta Sci. Circumst.* **2004**, *24*, 555–557.
54. Pant, R.R.; Zhang, F.; Rehman, F.U.; Wang, G.; Ye, M.; Zeng, C.; Tang, H. Spatiotemporal variations of hydrogeochemistry and its controlling factors in the Gandaki River Basin, Central Himalaya Nepal. *Sci. Total Environ.* **2018**, *622*, 770–782. [[CrossRef](#)]
55. Wu, W.H. Hydrochemistry of inland rivers in the north Tibetan Plateau: Constraints and weathering rate estimation. *Sci. Total Environ.* **2016**, *541*, 468–482. [[CrossRef](#)]
56. Zhang, Y.; Zhu, G.; Ma, H.; Yang, J.; Pan, H.; Guo, H.; Wan, Q.; Yong, L. Effects of Ecological Water Conveyance on the Hydrochemistry of a Terminal Lake in an Inland River: A Case Study of Qingtu Lake in the Shiyang River Basin. *Water* **2019**, *11*, 1673. [[CrossRef](#)]
57. Li, Q.; Wu, J.; Shen, B.; Zeng, H.; Li, Y. Water Chemistry and Stable Isotopes of Different Water Types in Tajikistan. *Environ. Process.* **2018**, *5*, 127–137. [[CrossRef](#)]
58. Meybeck, M. Global chemical weathering of surficial rocks estimated from river dissolved loads. *Am. J. Sci.* **1987**, *287*, 401–428. [[CrossRef](#)]
59. Ma, L.; Abuduwaili, J.; Li, Y.; Abdyzhaparuulu, S.; Mu, S. Hydrochemical Characteristics and Water Quality Assessment for the Upper Reaches of Syr Darya River in Aral Sea Basin, Central Asia. *Water* **2019**, *11*, 1893. [[CrossRef](#)]
60. Thomas, J.; Joseph, S.; Thirivikramji, K.; Manjusree, T.; Arunkumar, K. Seasonal variation in major ion chemistry of a tropical mountain river, the southern Western Ghats, Kerala, India. *Environ. Earth Sci.* **2014**, *71*, 2333–2351. [[CrossRef](#)]



© 2019 by the authors. Licensee MDPI, Basel, Switzerland. This article is an open access article distributed under the terms and conditions of the Creative Commons Attribution (CC BY) license (<http://creativecommons.org/licenses/by/4.0/>).